Kinetic Slip Condition, van der Waals Forces, and Dynamic Contact Angle

Len M. Pismen* and Boris Y. Rubinstein

Department of Chemical Engineering, Technion—Israel Institute of Technology, Haifa 32000, Israel

Received October 16, 2000. In Final Form: May 11, 2001

The profiles of a spreading wetting film are computed taking into account intermolecular forces and introducing a kinetic slip condition at a molecular cutoff distance. This eliminates the stress singularity, so that both "true" and "visible" contact angles are defined unequivocally. The true contact angle at the cutoff distance depends on the slip length as well as on the edge propagation speed but not on gravity or asymptotic inclination angle. These macroscopic factors influence, however, the visible contact angle observed in the interval where the actual film profile departs from the intermediate asymptotic curve.

I. Introduction

The two basic unsolved problems in the theory of a moving three-phase contact line are defining the contact angle and resolving the infamous viscous stress singularity. Different approaches to both problems, neither of them satisfactory, have been reviewed by Shikhmurzaev.[1] Even under equilibrium conditions, the structure of the three-phase region cannot be understood without taking into account intermolecular interactions between the fluid and the solid support.[2−4] It becomes apparent that motion of a contact line is an intrinsically *mesoscopic* problem, and the dynamical theory should blend factors contributed by hydrodynamics and physical kinetics.

The "standard" equilibrium contact angle θ_e is defined by the Young−Laplace formula

$$\sigma_v - \sigma_l = \sigma \cos \theta_e \tag{1}$$

which involves surface tension σ of an interface between two semi-infinite fluid phases (in the simplest case, a one-component liquid and its vapor) and (nonmeasurable) surface tensions between the solid support and either fluid, σ_l and σ_v. Since, by definition, the standard surface tension refers to a boundary between semi-infinite phases, the surface properties should be modified when the three-phase region falls within the range of intermolecular forces, and therefore the classical formula is likely to fail in a close vicinity of the contact line. This region is too small to be detected by available measurement techniques, but modification of interfacial properties is often revealed by the formation of a precursor film. Thus, even under equilibrium conditions the contact angle, generally, varies with the distance from the contact line and cannot be defined unequivocally.

In a dynamical situation, such as wetting, spreading, or drawdown of a meniscus, the interfacial curvature and hence the change of the contact angle are further influenced by the viscous stress. A properly defined contact angle fixes the boundary condition at the edge of an advancing or receding film and is therefore a necessary ingredient for computation of macroscopic flows, influenced also by external forces, such as gravity, and by changes in temperature and chemical composition through buoyancy and Marangoni effect. Macroscopic measurements yield the so-called "visible" contact angle, differing from both the standard value in eq 1 and a hypothetical "true" (microscopic) value. Both true and visible contact angles should depend on the flow velocity and are subject to hysteresis.

One should be warned that the very notion of a true interfacial angle is precarious, since it extrapolates the concept of a sharp interface of a continuous theory to molecular distances. This notion is eliminated altogether in molecular simulations[5,6] and in diffuse interface theories.[7−10] In continuum theories incorporating intermolecular forces, the true contact angle can be defined *at most* at the molecular cutoff distance d. This is sometimes forgotten when hydrodynamic theory leads to the appearance of unphysically narrow boundary layers.

Bearing in mind limitations of continuum mechanics extended to molecular scales, we attempt in this communication to combine the standard hydrodynamic theory with a simple kinetic description of sliding motion in the first molecular layer adjacent to the solid support. The thickness of the sliding layer is identified with the cutoff length in the van der Waals interaction potential; thus, the theory is expected to operate at about the same crude level as the classroom derivation of the van der Waals equation of state.[11]

The paper is organized as follows. We start in section II with a detailed discussion of the slip condition. Basic equations in lubrication approximation are formulated in

(1) Shikhmurzaev, Yu. D. Moving contact lines in liquid/liquid/solid systems. *J. Fluid Mech.* **1997**, *334*, 211.
(2) Derjaguin, B. V.; Churaev, N. V.; Muller, V. M. *Surface Forces*; Consultants Bureau: New York, 1987.
(3) Israelachvili, J. H. *Intermolecular and Surface Forces*; Academic Press: New York, 1992.
(4) de Gennes, P. G. Wetting: statics and dynamics. *Rev. Mod. Phys.* **1985**, *57*, 827.
(5) Koplik, J.; Banavar, J. R.; Willemsen, J. F. Molecular dynamics of a fluid flow at solid surfaces. *Phys. Fluids A* **1989**, *1*, 781.
(6) Thompson, P. A.; Robbins, M. O. Simulations of contact-line motion: slip and the dynamic contact angle. *Phys. Rev. Lett.* **1989**, *63*, 766.
(7) Anderson, D. M.; McFadden, G. B.; Wheeler, A. A. Diffuse-interface methods in fluid mechanics. *Annu. Rev. Fluid Mech.* **1998**, *30*, 139.
(8) Merchant, G. J.; Keller, J. B. Contact angles. *Phys. Fluids* **1992**, *A4*, 477.
(9) Seppecher, P. Moving contact lines in the Cahn-Hilliard theory. *Int. J. Eng. Sci.* **1996**, *34*, 977.
(10) Pismen, L. M.; Pomeau, Y. Disjoining potential and spreading of thin liquid layers in the diffuse interface model coupled to hydrodynamics. *Phys. Rev. E* **2000**, *62*, 2480.
(11) Landau, L. D.; Lifshitz, E. M. *Statistical Physics*; Pergamon Press: 1980.

10.1021/la001452s CCC: $20.00
Published on Web 07/27/2001

section III. Intermediate asymptotics of the solutions at relatively short macroscopic distances from the contact line, where gravity still does not come into play, are discussed in section IV. Solutions describing the form of a stationary meniscus on a moving inclined plane are given in section V.

II. Slip Condition

With any finite contact angle given as a boundary condition, a moving contact line still cannot be described within the framework of conventional hydrodynamics, since the classical no-slip condition on a solid substrate generates a multivalued velocity and, hence, an infinite stress in the vicinity of a contact line, leading formally to an infinite drag force.[12,13]

The most common way to eliminate the viscous stress singularity is to impose a phenomenological *slip* condition. Presence of slip at a microscopic scale comparable with intermolecular distances is an established fact in Maxwell's[14] kinetic theory of gases; for dense fluids, it is a feasible hypothesis supported by molecular dynamics simulations.[5,6] The two alternatives are slip conditions of the "hydrodynamic" and "kinetic" types.

The version of the slip condition most commonly used in fluid-mechanical theory is a linear relation between the velocity component along the solid surface u_s and the shear stress.[15,16] The proportionality constant contains a phenomenological parameter, slip length, characterizing intermolecular interaction between the fluid and the solid; in liquids, this length should be small, so that the effect of sliding becomes significant only in the vicinity of a moving contact line where stresses are very large. This condition has been widely used for modeling macroscopic flows involving the contact line motion.[17−21] It does not eliminate the stress singularity but only makes it integrable, thus leaving a logarithmic (integrable) singularity of the interfacial curvature. This leads formally to a breakdown of the commonly used lubrication approximation in the vicinity of a contact line that can be remedied only by further *ad hoc* assumptions, making the slip length dependent on the distance from the contact line.[18,21]

This drawback may be merely technical, but a more serious disadvantage of hydrodynamic slip theories lies in their inherent inability to predict the dynamic contact angle. Thus, the two basic problems become disentangled, and, in addition to a phenomenological slip coefficient, empirical relationships between the velocity and contact angle have to be introduced in model computations.

Another version of the slip condition[22,23] defines the slip velocity through the gradient of thermodynamic potential w along the solid surface:

$$u_s = -\frac{D}{nkT}\nabla w \qquad (2)$$

where D is surface diffusivity, n is particle number density, k is the Boltzmann constant, T is temperature, and ∇ is the two-dimensional gradient operator along the solid surface. The condition in (2) is rooted in physical kinetics and follows rather naturally from considering activated diffusion in the first molecular layer adjacent to the solid.[24,25] In contrast to the hydrodynamic slip condition, the kinetic condition in (2) can be used to define the true dynamic contact angle at the contact line in a unique way, as we shall see below.

Extrapolating the continuous description of fluid motion to a molecular scale might be conceptually difficult but unavoidable as far as interfacial dynamics is concerned. Long-range intermolecular interactions, such as London−van der Waals forces, still operate on a mesoscopic scale where continuous theory is justified, but they should be bounded by an inner cutoff d of atomic dimensions. Thus, distinguishing the first molecular layer from the bulk fluid becomes necessary even in equilibrium theory. In dynamic theory, the motion in the first molecular layer can be described by eq 2, whereas the bulk fluid obeys hydrodynamic equations supplemented by the action of intermolecular forces. Equation 2 serves then as the boundary condition at the solid surface. Moreover, at the contact line, where the bulk fluid layer either terminates altogether or gives way to a monomolecular precursor film, the same slip condition defines the slip component of the flow pattern, and eq 2 can be used to estimate the true contact angle if it is assumed that the motion is pure slip at the contact line.

Miller and Ruckenstein[26] used the dependence of the disjoining pressure generated by London−van der Waals forces in a wedge to compute the true equilibrium contact angle. This result has been used by Hocking[27] to set the boundary condition at the contact line in the hydrodynamic theory. Order-of-magnitude estimates show, however, that at small inclination angles necessary to justify the lubrication approximation used in hydrodynamic theory the correction to disjoining pressure due to surface inclination is extremely small, and the true angle may be formally attained only at distances far below atomic dimensions. At higher inclination angles, the computation fails technically, since the interface must be curved, and its form should be determined by a very complicated integro-differential equation involving intermolecular interactions as well as viscous stress and surface tension.

Ruckenstein and Dunn[22] computed the slip velocity by combining eq 2 with the same expression for the disjoining pressure in a wedge, with the intention to use the dependence $u_s(h)$ obtained in this way for hydrodynamic theory in lubrication approximation. We propose to use the kinetic slip condition in the another way and, rather than fixing the true contact angle through an equilibrium condition in a wedge,[26] compute it dynamically by balancing the London−van der Waals forces and viscous dissipation in a thin precursor film. In this way, we shall

(12) Huh, C.; Scriven, L. E. Hydrodynamical model of steady movement of a solid/liquid/fluid contact line. *J. Colloid Interface Sci.* **1971**, *35*, 85.
(13) Dussan, E. B.; Davis, V. S. H. On the motion of a fluid-fluid interface along a solid surface. *J. Fluid Mech.* **1974**, *65*, 71.
(14) Maxwell, J. C. *Philos. Trans. R. Soc. London, Ser. A* **1867**, *70*, 231.
(15) Lamb, H. *Hydrodynamics*; Dover: 1932.
(16) Bedeaux, D.; Albano, A. M.; Mazur, P. Boundary conditions and nonequilibrium thermodynamics. *Physica A* **1976**, *82*, 438.
(17) Hocking, L. M. A moving fluid interface. Part 2. The removal of the force singularity by a slip flow. *J. Fluid Mech.* **1977**, *79*, 209.
(18) Greenspan, H. P. On the motion of a small viscous droplet that wets a surface. *J. Fluid Mech.* **1978**, *84*, 125.
(19) Hocking, L. M. The spreading of a thin drop by gravity and capillarity. *Q. J. Mech. Appl. Math.* **1981**, *34*, 55.
(20) Hocking, L. M. Spreading and instability of a viscous fluid sheet. *J. Fluid Mech.* **1990**, *211*, 373.
(21) Haley, P. J.; Miksis, M. J. The effect of the contact line on droplet spreading. *J. Fluid Mech.* **1991**, *223*, 57.
(22) Ruckenstein, E.; Dunn, C. S. Slip velocity during wetting of solids. *J. Colloid Interface Sci.* **1977**, *59*, 135.
(23) Ruckenstein, E. The moving contact line of a droplet on a smooth solid. *J. Colloid Interface Sci.* **1995**, *170*, 284.
(24) Blake, T. D.; Haynes, J. M. Kinetics of liquid−liquid displacement. *J. Colloid Interface Sci.* **1969**, *30*, 421.
(25) Brochard-Wyart, F.; de Gennes, P. G. Dynamics of partial wetting. *Adv. Colloid Interface Sci.* **1992**, *39*, 1.
(26) Miller, C. A.; Ruckenstein, E. The origin of flow during wetting of solids. *J. Colloid Interface Sci.* **1974**, *48*, 368.
(27) Hocking, L. M. The influence of intermolecular forces on thin fluid layers. *Phys. Fluids A* **1993,** *5*, 793.

obtain a relation between the slip velocity and the thermodynamic potential at the contact line by considering the motion at the point where the film thins down to the minimal thickness $h = d$. This is the advancing edge of a wetting film or a retreating edge of a dewetting film, dividing it from the dry solid surface. If the fluid is not volatile, the motion at this point should be pure slip, while standard caterpillar motion is retained at observable macroscopic distances. In the case of an advancing wetting film, we expect that the leading edge is followed by a thin precursor film where surface tension is negligible and the action of intermolecular forces driving the advancing film is balanced by viscous dissipation. The boundary condition at the leading edge will be then the same eq 2 with u_s replaced by the edge propagation speed U and ∇w computed at $h = d$ with surface tension neglected.

We shall also check (and eventually dismiss) another way to construct a boundary condition at the leading edge, assuming that the slip motion at the edge is driven by the potential drop over the molecular cutoff distance d. This yields, by analogy with eq 2, the boundary condition at the contact line

$$U = -\frac{D}{nkT}\frac{w(d)}{d} \tag{3}$$

where $w(d)$ is the thermodynamic potential of the film of the minimal thickness; the potential at the dry surface is taken as zero. After $w(d)$ is computed as in the following section, eq 3 turns into a condition relating the curvature at the contact line with the propagation speed. We shall see that this condition leads in fact to nonphysical results at small propagation velocities. At large velocities, computations using the alternative boundary conditions yield practically the same results (see section IV).

III. Basic Equations and Scaling

We shall use the lubrication approximation, which is formally obtained by scaling the two-dimensional gradient operator along the solid surface $\nabla \propto \epsilon, \epsilon \ll 1$. Respectively, time is scaled as $\partial_t \propto \epsilon^2$; the velocity in the direction parallel to the solid support, as $u \propto \epsilon$; and transverse velocity, as $u \propto \epsilon^2$. This implies that the thermodynamic potential w is constant across the layer. The gradient of w in the direction parallel to the solid support serves as the forcing term in the Stokes equation. The velocity profile $u(z)$ across the film verifies

$$\nabla w = \eta u_{zz} \qquad u_z(h) = 0 \qquad u(d) = u_s \tag{4}$$

where η is the dynamic viscosity. We use here the no-stress boundary condition on the free surface $z = h$ but replace the usual no-slip boundary condition on the solid support $u(0) = 0$ by the slip condition at the molecular cutoff distance d with u_s given by eq 2. The solution in the bulk layer $d < z < h$ is

$$u = -\eta^{-1}\left[\lambda^2 + h(z - d) - \frac{1}{2}(z^2 - d^2)\right]\nabla w \tag{5}$$

where $\lambda = \sqrt{D\eta/nkT}$ is the effective slip length.

The general balance equation for the film thickness h, obtained from the kinematic condition on the free surface, can be presented as a generalized Cahn−Hilliard equation, where the two-dimensional flux $\mathbf{j}$ in the plane aligned with the solid support is proportional to the two-dimensional gradient of the potential w:

$$h_t + \nabla\cdot\mathbf{j} = 0 \qquad \mathbf{j} = -\eta^{-1}Q(h)\,\nabla w \tag{6}$$

The effective mobility $\eta^{-1}Q(h)$ is obtained by integrating eq 5 across the layer. Including also the constant slip velocity $u = -\lambda^2\eta^{-1}\nabla w$ in the slip layer $0 < z < d$, we have

$$Q(h) = \left[\lambda^2 h + \frac{1}{3}(h - d)^3\right] \tag{7}$$

Since both λ and d are measurable on the molecular scale (see the estimates in the end of this section), this expression does not differ in a macroscopically thick layer from the standard shallow water mobility $Q_0 = (1/3)h^3$, and the correction becomes significant only in the immediate vicinity of the contact line.

The potential w is computed at the free surface $z = h$. Taking into account surface tension, gravity, and van der Waals force, it is expressed as

$$w = -\sigma\epsilon^2\nabla^2 h + g\rho(h - \alpha x) - \frac{A}{6\pi h^3} \tag{8}$$

where A is the Hamaker constant, g is acceleration of gravity, ρ is density, σ is surface tension, and $\epsilon\alpha$ is the inclination angle of the solid surface along the x axis. The dummy small parameter ϵ is the ratio of characteristic scales across and along the layer; the relative scaling of different terms in eq 8 is formally consistent when $\sigma = O(\epsilon^{-2})$. Further on, we suppress the dependence on the second coordinate in the plane, replacing the Laplacian by $\mathrm{d}^2/\mathrm{d}x^2$.

In the following, we shall consider the film with a contact line steadily advancing along the x axis in the negative direction with the speed U. Then, eq 6 can be rewritten in the comoving frame, thus replacing h_t by Uh_x, and integrated once. Making use of the condition of zero flux through the contact line to remove the integration constant yields

$$-\eta U h + Q(h)\,w'(x) = 0 \tag{9}$$

This equation can be further transformed using h as the independent variable and $y(h) = h_x^2$ as the dependent variable. We rewrite the transformed equation introducing the capillary number $\mathrm{Ca} = |U|\eta/\sigma\epsilon^2$, van der Waals length $a = \epsilon^{-1}(|A|/6\pi\sigma)^{1/2}$, and gravity length $b = \epsilon(\sigma/g\rho)^{1/2}$:

$$\frac{h\mathrm{Ca}}{\sqrt{y}\,Q(h)} + \frac{1}{2}y''(h) - \frac{3a^2}{h^4} - \frac{1}{b^2}\left(1 - \frac{\alpha}{\sqrt{y}}\right) = 0 \tag{10}$$

The boundary condition following from (2) and balancing intermolecular forces and viscous dissipation at $h = d$ takes the form

$$y(d) = (d^4\mathrm{Ca}/3\lambda^2a^2)^2 \tag{11}$$

The alternative boundary condition in (3), set at $h = d$, is rewritten, using eq 8 and neglecting the gravity term, as

$$\frac{1}{2}y'(d) = \frac{d\mathrm{Ca}}{\lambda^2} - \frac{a^2}{d} \tag{12}$$

Equation 10 contains three microscopic scales d, a, and λ and a macroscopic gravity length b. The natural choice for d is the nominal molecular diameter, identified with the cutoff distance in the van der Waals theory. The standard value[3] is 0.165 nm. The slip length is likely to be of the same order of magnitude. The approximate

relation between viscosity η and self-diffusivity D_m in a liquid[28] yields $D_m\eta \approx 10^2 kT/3\pi d$. The surface diffusivity should be somewhat lower than the diffusivity in the bulk liquid, and with $D/D_m \approx 0.1$ we have $\lambda \approx d$.

The van der Waals length a depends on the relative strength of liquid−liquid and liquid−solid interactions. The Hamaker constant for the pair fluid−solid is defined[3] as

$$A = \pi^2 n(C_s n_s - C_f n) \equiv \pi^2 n^2 \tilde{C} \tag{13}$$

where C_s and C_f are constants in the long-range attraction potential C/r^6 for the pairs of fluid−solid and fluid−fluid atoms, respectively, removed at the distance r; n_s is the solid number density. The effective interaction parameter $\tilde{C}$ is defined by the above identity. We shall assume $A > 0$, which corresponds to the case of complete wetting. The estimate for surface tension[3] is $\sigma \approx (1/24)\pi C_f (n/d)^{-2}$. This gives $a \approx 2\epsilon^{-1}(\tilde{C}/C_f)^{1/2}$, so that $a = O(d)$ when $\tilde{C}/C_f = O(\epsilon^2)$.

IV. Intermediate Asymptotics

In the intermediate region, where h far exceeds the microscopic scales d, a, and λ but is still far less than the capillary length b, the film profile is determined by the balance between viscous stress and surface tension. The asymptotics of the truncated eq 10 (with d, a, λ, and b^{-1} set to zero) at $h \to \infty$ is

$$y \approx \left(3\mathrm{Ca}\ln\frac{h}{h_0}\right)^{2/3} - 2\left(\frac{\mathrm{Ca}}{9}\right)^{2/3}\ln\ln\frac{h}{h_0}\left(\ln\frac{h}{h_0}\right)^{-1/3} + \ldots \tag{14}$$

where h_0 is an indefinite constant. The first term of this asymptotic expression has been obtained by Hervet and de Gennes,[29] who have also reported the value of h_0. This constant can be obtained by integrating eq 10 (with gravity neglected) starting from the boundary condition in (11) or (12) and adjusting another necessary boundary value to avoid runaway to $\pm\infty$. There is a unique heteroclinic trajectory approaching the asymptotics (14). It is very sensitive to the initial conditions as well as to the molecular-scale factors operating close to the contact line. The growth of the inclination angle is never saturated, as long as macroscopic factors (gravity or volume constraint) are not taken into account.

Equation 10 can be integrated using the shooting method: either starting from the boundary condition in (11) and adjusting $y'(d)$ or starting from the boundary condition in (12) and adjusting $y(d)$ to arrive at the required asymptotics at $h \to \infty$. Further on, we will measure all lengths in the molecular units and set d to unity. The solution in the intermediate region depends on the physical parameters a and λ as well as on the capillary number Ca that includes the propagation speed U. The latter's impact is most interesting for our purpose. Examples of the computed dependence of the inclination angle $\theta = \sqrt{y(h)}$ on the local film thickness h using the boundary condition in (11) at different values of Ca are given in Figure 1a.

The curves in Figure 1b using the boundary condition in (12) show peculiar (apparently nonphysical) reversal of the dependence of the inclination angle on Ca, resulting in an *increase* of the true contact angle $\theta(d)$ with decreasing velocity. Indeed, at $U \to 0$ this condition yields a spurious balance between intermolecular forces and surface tension leading to an *unstable* stationary state, similar to the erroneous inference of a wetting film with the right contact angle in ref 30 discussed in our earlier paper.[31] The anomaly, however, quickly disappears at observable distances.

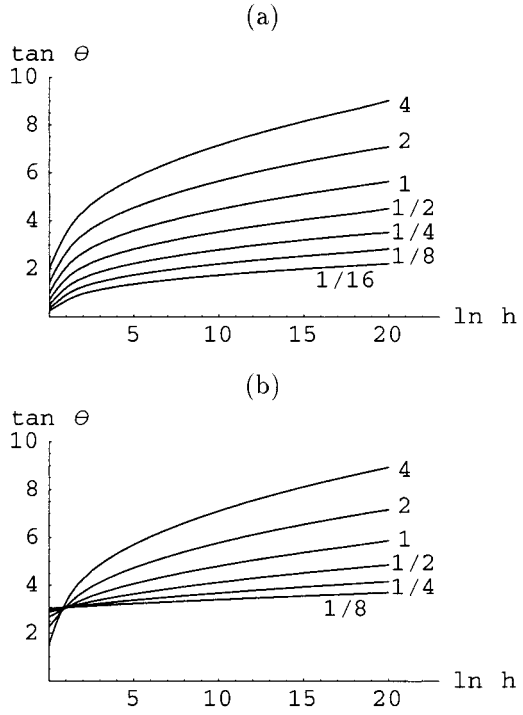

Figure 1. Dependence of the local surface inclination tan θ on the local film thickness at different values of the capillary number Ca computed using the boundary condition in (11) (a) and (12) (b). The numbers at the curves show the values of Ca. Other parameters used in all computations are $\lambda = 1$ and $a = 1/\sqrt{3}$.

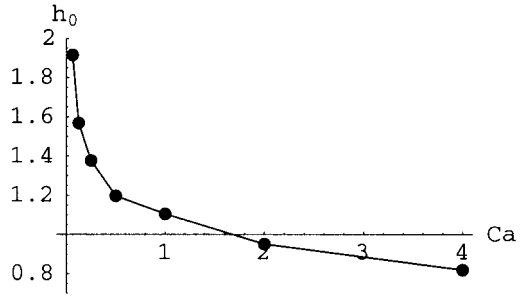

Figure 2. Dependence of h_0 on Ca computed using the data from Figure 1a.

The curve segments at $h \gg 1$ can be fit to the asymptotic formula in (14) to obtain the integration constant h_0. The asymptotic formula in (14) can be used only when h is *logarithmically* large, and the convergence, as estimated by the second term, is slow; therefore, h_0 can be only obtained approximately from the computed profiles. The dependence of h_0 on Ca based in Figure 1a is shown in Figure 2. We see here a rather strong variation of the integration constant, unlike a single "universal" value reported in ref 29.

V. Drawdown of a Meniscus

The simplest stationary arrangement including gravity is realized when an inclined plane, dry at $x \to -\infty$, slides

(28) Frenkel, Ia. I. *Kinetic Theory of Liquids*; Clarendon Press: Oxford, 1946.

(29) Hervet, H.; de Gennes, P. G. The dynamics of wetting: precursor films in the wetting of 'dry' solids. *C. R. Acad. Sci.* **1984**, *299 II*, 499.

(30) de Gennes, P. G.; Hue, X.; Levinson, P. Dynamics of wetting: local contact angles. *J. Fluid Mech.* **1990**, *212*, 55.

(31) Pismen, L. M.; Rubinstein, B. Y.; Bazhlekov, I. Spreading of a wetting film under the action of van der Waals forces. *Phys. Fluids* **2000**, *12*, 480.

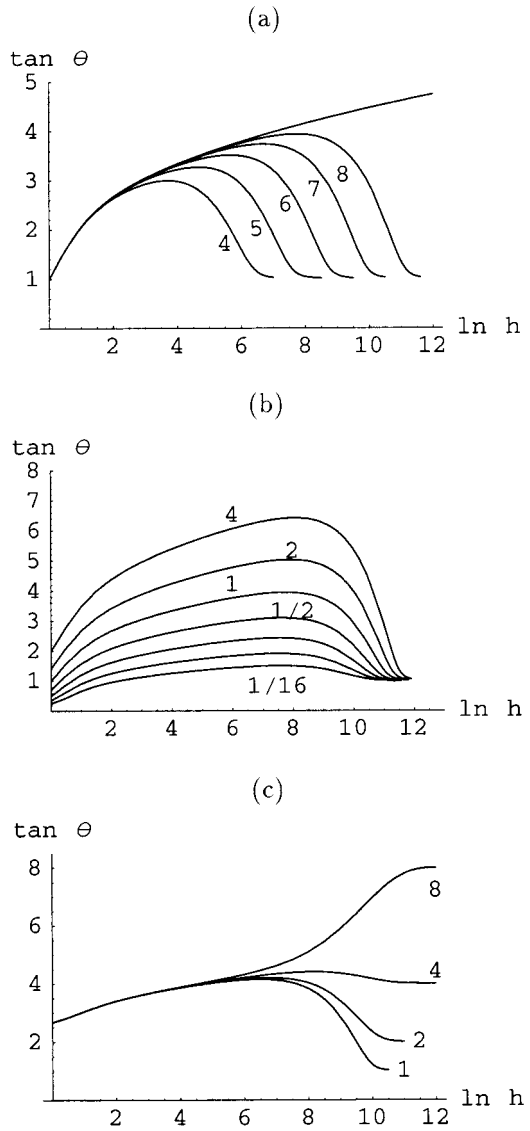

Figure 3. Dependence of the local surface inclination angle θ on the film thickness (a) at Ca = 1, $\alpha = 1$, and different values of the gravity length b; (b) at $b = 10^4$ and different values of the capillary number Ca; (c) at Ca = 1, $b = 10^4$, and different values of the asymptotic inclination angle α. The numbers at the curves show the values of (a) 2 log b, (b) Ca, and (c) α. Other parameters used in all computations are $\lambda = 1$ and $a = 1/\sqrt{3}$.

in the direction of a wetting layer. Solving eq 10 with the same boundary condition in (12) as before brings now to the asymptotics $y = \sqrt{\alpha}$ at $h \rightarrow \infty$ that corresponds to a horizontal layer.

The curves $y(h)$ seen in Figure 3a,c all depart from the intermediate asymptotic curve obtained for infinite b as in the preceding section. However, due to extreme sensitivity of the shooting method to the choice of the missing initial value, one has to integrate from the outset the full equation rather than trying to start integration from some point on the intermediate asymptotic curve. One can see that the maximum inclination angle (which may be identified with the visible contact angle) grows as b decreases. This increase is, however, not pronounced when the initial incline (identified with the true contact angle) is high. One can distinguish therefore between two possibilities: first, when the main dissipation is due to kinetic resistance in the first monomolecular layer that raises $y(d)$ and, second, when the viscous dissipation

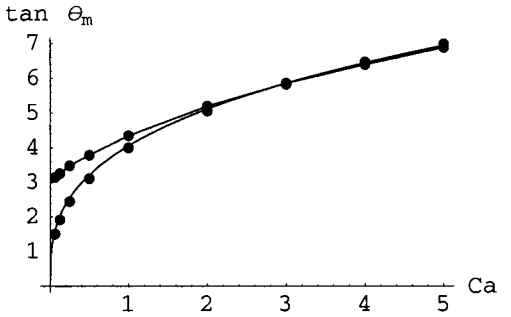

Figure 4. Dependence of the visible contact angle θ_m on Ca.

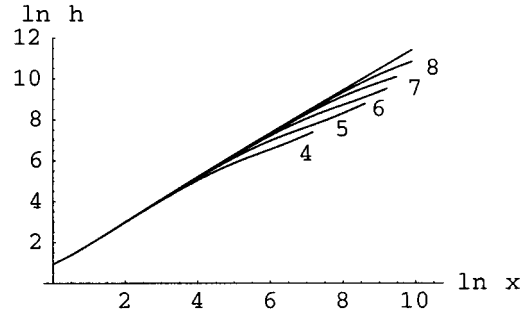

Figure 5. The shape of the meniscus for different values of b. The numbers at the curves show the values of 2 log b.

prevails and the inclination angle keeps growing in the region of bulk flow. Take note that even in the latter case the region where the inclination and curvature are high is close to the contact line when measured on a macroscopic scale.

Figure 4 shows the dependence of the visible contact angle θ_m, defined as the maximum inclination angle and observed in the range where the gravity-dependent curves depart from the intermediate asymptotics, on the capillary number Ca. The lower curve is a fit $\theta \propto \mathrm{Ca}^{1/3}$ to the data of Figure 3b. The points of the upper curve are computed in a similar way using the boundary condition in (12). The first result appears to be more physically reasonable, since the angle drops close to zero at small flow velocities, while in the alternative computation it remains finite (see also the discussion in the preceding section). The proportionality of the inclination angle to $\mathrm{Ca}^{1/3}$ (which leads to the well-known Tanners law of spreading[4]) is a property of the intermediate asymptotics in (14) that can be deduced from scaling,[31] although the universality is slightly impaired by the dependence of the integration constant h_0 on velocity seen in Figure 2. The one-third law is inherited by the dependence $\theta_m(\mathrm{Ca})$, since the inclination angle reaches its maximum while the gravity-dependent profile is still close to the intermediate asymptotic curve.

Figure 5 shows the actual shape of the meniscus obtained by integrating the equation $h'(x) = \sqrt{y(h)}$, $h(0) = d$. The dependence of the drawdown length Δ (computed as the difference between the actual position of the contact line and the point where the continuation of the asymptotic planar interface hits the solid surface) on the gravity length is shown in Figure 6.

VI. Conclusion

It comes, of course, as no surprise that introducing a molecular cutoff and applying a kinetic slip condition to the first molecular layer resolves the notorious singularities of hydrodynamic description. The hydrodynamic singularities are eliminated, however, only at molecular distances and are still felt in sharp interface curvatures

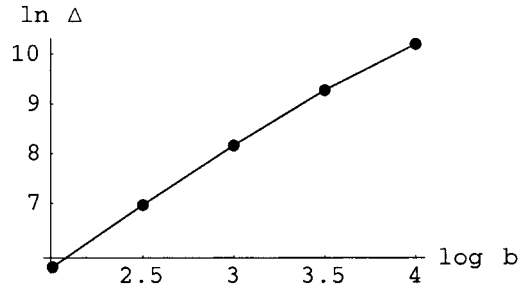

Figure 6. The dependence of the drawdown length Δ on log *b*.

at microscopic distances identified here as the intermediate asymptotic region. The computations are eased considerably when nonphysical divergence of both viscous stress and attractive Lennard-Jones potential beyond the cutoff limit are eliminated. As a result, the stationary equations can be solved by the shooting method with reasonable accuracy in a very wide range extending from molecular to macroscopic scales, and the true contact angle at the cutoff distance can be defined unequivocally.

The true angle (unobservable by available techniques) depends on the slip length as well as on the edge propagation speed but not on gravity or asymptotic inclination angle. These macroscopic factors influence, however, the visible contact angle observed in the interval where the actual film profile departs from the intermediate asymptotic curve. Since the latter's location, though not shape, depends on the molecular-scale factors as well as on the cutoff distance, the visible angle depends on both molecular and macroscopic factors. Thus, the lack of simple recipes for predicting the value of dynamic contact angle is deeply rooted in the mesoscopic character of the contact line.

Acknowledgment. This research has been supported by the Israel Science Foundation. L.M.P. acknowledges partial support from the Minerva Center for Nonlinear Physics of Complex Systems.

LA001452S